Control of Piecewise Linear Dynamics in Nonautonomous Hamiltonian Systems

Yannis Kominis and Tassos Bountis

Department of Mathematics
University of Patras

INCT DE SISTEMAS COMPLEXOS 5TH WORKSHOP
CBPF, RIO DE JANEIRO, 22 - 24 APRIL, 2013

Summary of the Talk

1. We focus on Hamiltonian systems consisting of **a periodic sequence of linear and nonlinear autonomous components** and focus on the **control of their dynamics**.

2. Choosing the **lengths of the linear and nonlinear intervals** accordingly, we **continue analytical solutions** of the nonlinear components across the linear intervals.

3. We demonstrate these ideas on **a Duffing equation and a 1-dimensional Toda lattice**, with periodically switched on-off coefficients and analytically continue **homoclinic (heteroclinic) solutions** in the former and **solitons** in the latter.

4. We obtain exact **traveling Solitary Waves** (SW) for a variety of **inhomogeneous optical structures** consisting of linear and nonlinear layers, in the **non-paraxial regime**, with many applications.

Introduction

Nonautonomous dynamical systems are commonly used as models for a large variety of natural or man-made systems, in which **the independent variable is time or space**.

(a) In the first category we have **forced oscillators** and **oscillators with time-varying parameters**.

(b) In the second we find **spatially inhomogeneous models**, that describe periodic or solitary wave formation in **inhomogeneous structures**.

We use **piecewise constant periodic functions** in periodic arrays of autonomous linear and nonlinear elements acting over **different space intervals**. Our aim is to vary parameters and **change phase space topology** so as to control soliton propagation.

The Duffing model

We consider a **nonautonomous Hamiltonian system** consisting of a **nonlinear autonomous** one degree of freedom component, **interrupted periodically by a linear component** of frequency ω_0. The overall period is $T = T_N + T_L$ with T_N, T_L being the durations of time intervals in which the nonlinear and linear systems, respectively, act alone. The Hamiltonian of the total system has the form

$$H = \frac{p^2}{2} + f(t)\frac{q^2}{2} + g(t)\frac{q^4}{4} \tag{1}$$

where the piecewise constant functions f and g are defined as

$$[f(t), g(t)] = \begin{cases} [\mp 1, \pm 1], & \text{if } t \in [kT, (k+1)T - T_L) \\ [\omega_0^2, 0], & \text{if } t \in [(k+1)T - T_L, (k+1)T), \end{cases} \qquad k = \tag{2}$$

In such nonautonomous systems, **drastic changes on the topology of the phase space** are expected as the duration of the action of the linear system T_L increases from zero. First of all, it has been shown that a Poincare surface of section of the **nonautonomous system is identical to the phase space of the autonomous nonlinear system** when T_L is equal to an integer multiple of the half-period of the linear system,

$$T_L^{(n)} = n\frac{\pi}{\omega_0}, \qquad n = 1, 2, 3, ... \tag{3}$$

and families of nonlinear periodic, quasiperiodic and localized **solutions can be analytically obtained**. Here, we study the changes of the phase space for various values of T_L and investigate possible **control of the dynamics**, as we vary ω_0, T_L, and T_N.

Results

The nonlinear part of the system is described by the autonomous Hamiltonian

$$H_N = \frac{p^2}{2} \mp \frac{q^2}{2} \pm \frac{q^4}{4} \tag{4}$$

with the two signs denoting **Cases A and B**. H_N has three fixed points $O = (0, 0)$ and $P_{\pm 1} = (\pm 1, 0)$. In **Case A the origin is a saddle** connected to itself by a closed homoclinic orbit formed by the stable and unstable manifolds, while $P_{\pm 1}$ are centers. **The opposite is true in Case B**.

The dynamics can be studied via a **Poincare surface of section** at multiples of $t = T_N/2$. For small T_L the saddle fixed points of the system persist on the Poincare map as unstable periodic orbits, while their invariant manifolds intersect transversely. As T_L increases the topology of the phase space changes drastically.

The dynamics of Case A: The origin is a saddle point

Let us follow the modification of the dynamics on a Poincare surface of section as T_L is varied. In all cases we take $T_N = 1$, $\omega_0 = \pi$ while T_L varies in the interval $(0, T_L^{(1)})$.

In Figure 1, the Poincare surface of sections for different values of T_L is shown for Case A. **When $T_L = 0$, as well as when $T_L = T_L^{(n)}$ [Eq. (3)] the Poincare surface of section coincides with the phase portrait of the autonomous nonlinear system** H_N [Fig. 1(a)]. For small values of T_L the linear part does not alter the stability of the origin, as shown in Fig. 1(b). However, **the stable and unstable manifolds intersect transversely** at homoclinic points.

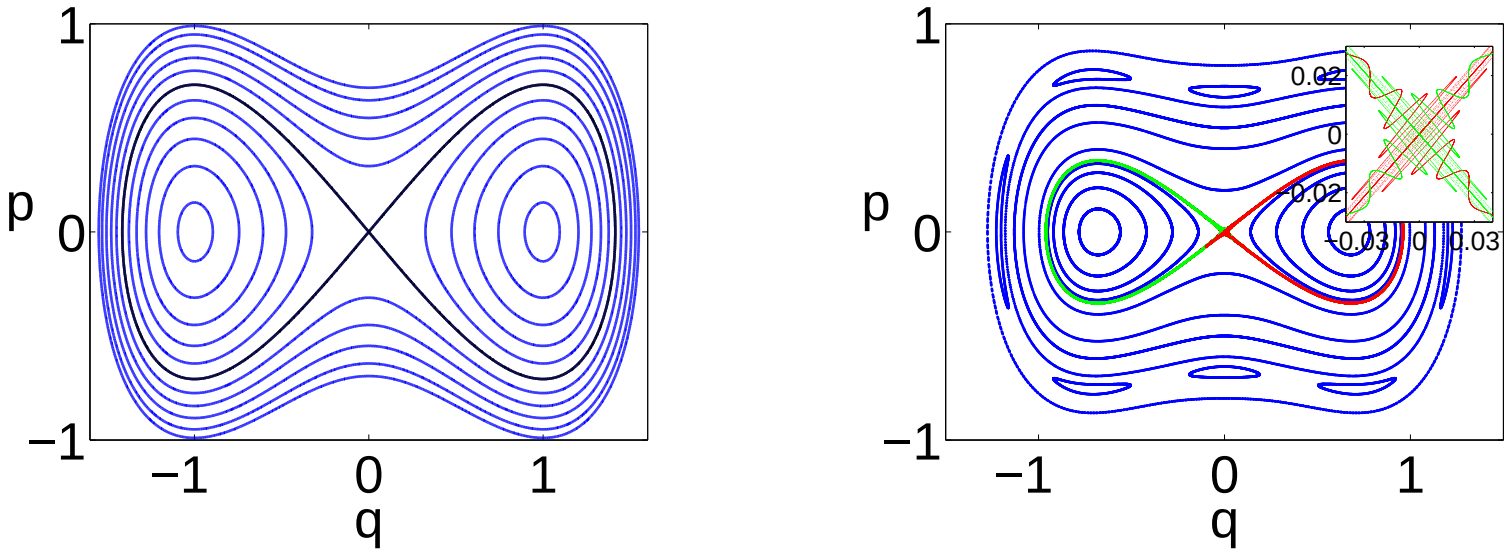

Figure 1 a,b: Poincare surface of section at $t = T_N/2$ for Case A. $\omega_0 = \pi$, $T_N = 1$, (a) $T_L = 0$, (b) $T_L = 0.05$. Red and green lines depict the unstable and stable manifolds.

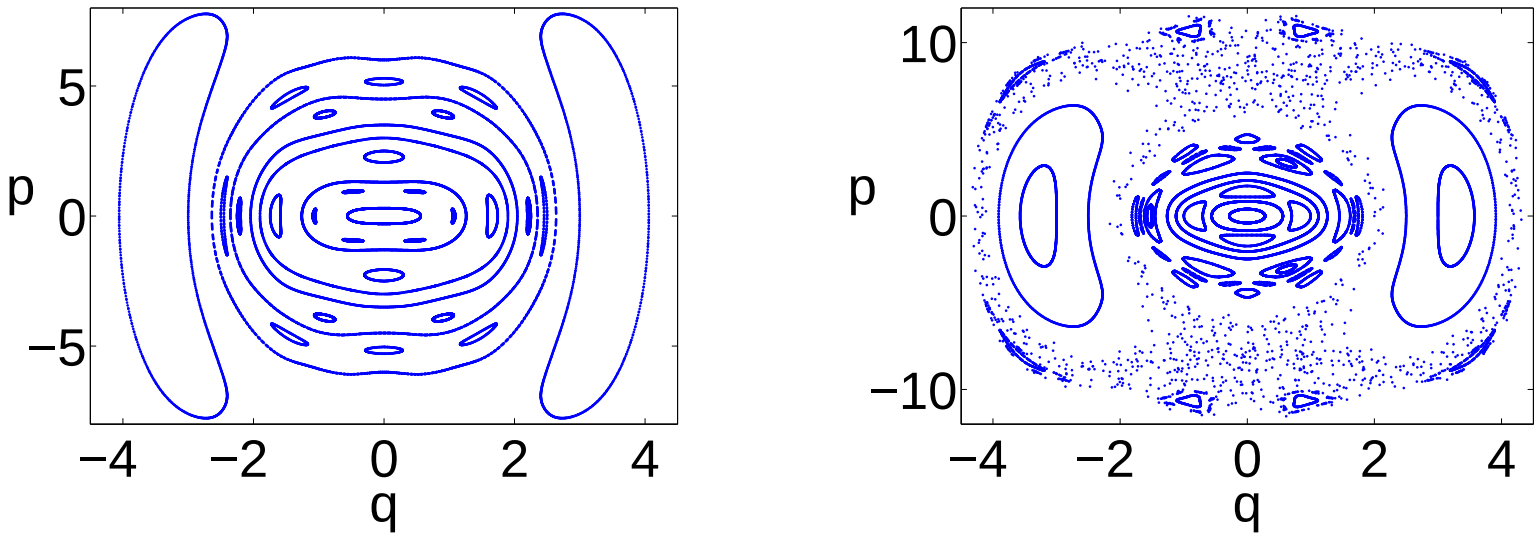

Figure 1 c,d: Poincare surface of section at $t = T_N/2$ for Case A. $\omega_0 = \pi$, $T_N = 1$, (c) $T_L = 0.1$, (d) $T_L = 0.2$.

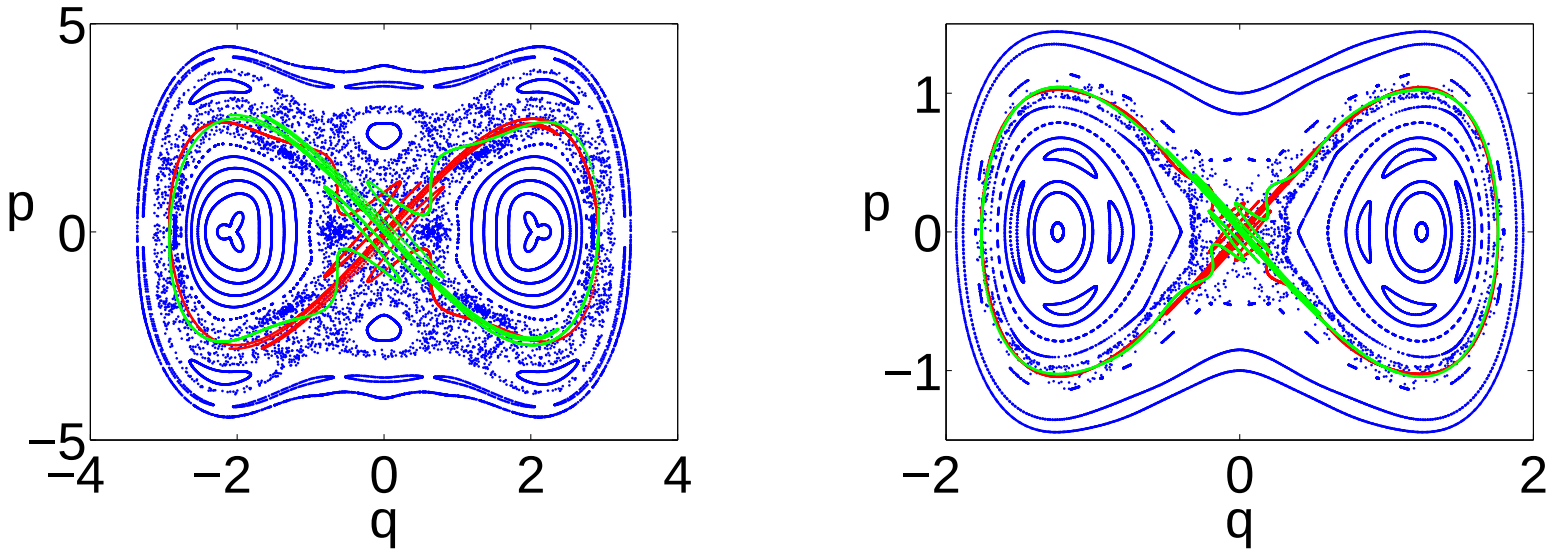

Figure 1 e,f: Poincare surface of section at $t = T_N/2$ for Case A. $\omega_0 = \pi$, $T_N = 1$, (e) $T_L = 0.7$, (f) $T_L = 0.95$. Red and green lines depict the unstable and stable manifolds.

The dynamics of Case B: The origin is an elliptic point

Small values of T_L do not alter the stability type of the origin, but **significantly increase the area** occupied by bounded quasiperiodic orbits (Fig. 2(a,b)). For $T_L \in (0.336, 0.890)$ the origin becomes a saddle **corresponding to a bright soliton**.

For $T_L = 0.35$ the homoclinic tangles are restricted in the vicinity of the origin, as shown in Fig. 2(d). However, for $T_L > 0.890$ the origin becomes again a center as shown in Fig. 2(f) and the phase portrait returns to the form shown in Fig. 2(a).

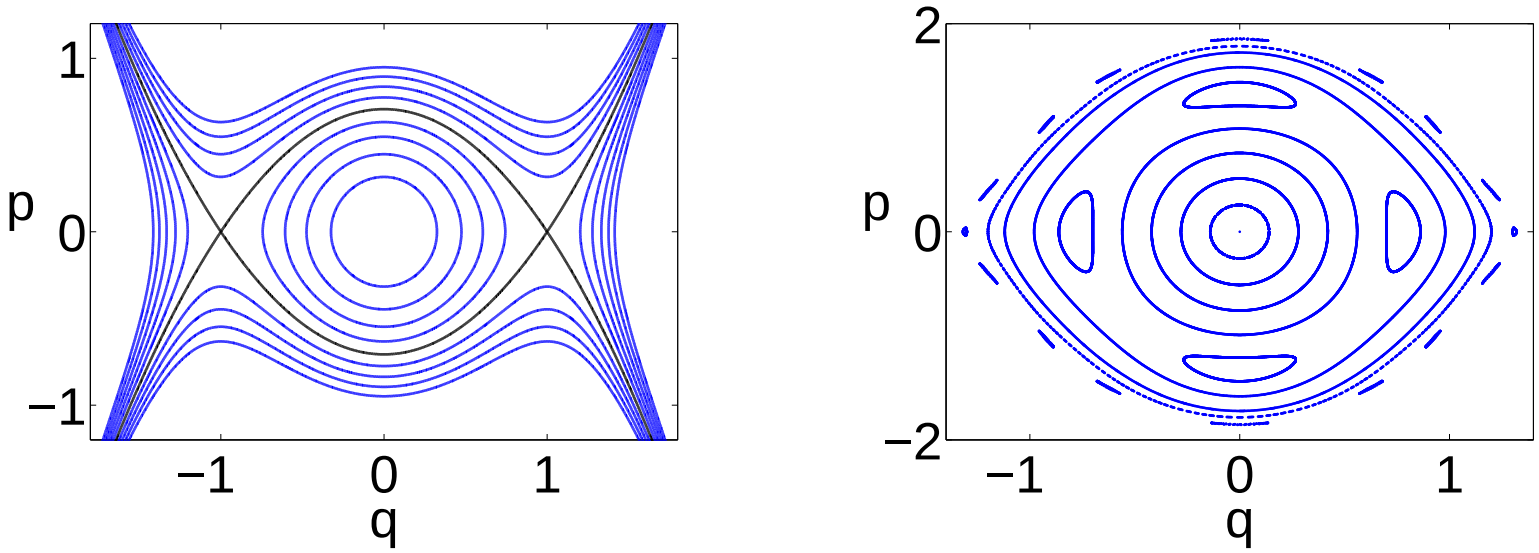

Figure 2 a,b: Poincare surface of section at $t = T_N/2$ for Case B. $\omega_0 = \pi$, $T_N = 1$, (a) $T_L = 0$, (b) $T_L = 0.15$. Black line in (a) depicts the heteroclinic orbit. Red and green lines depict the unstable and stable manifolds.

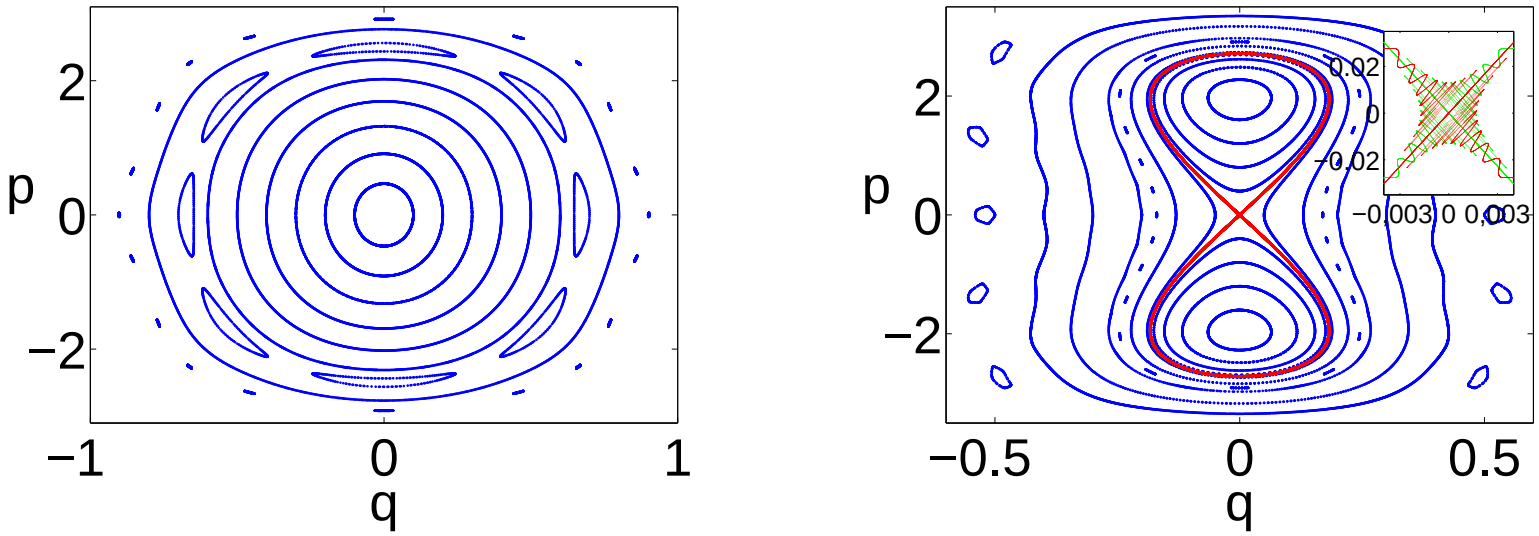

Figure 2 c,d: Poincare surface of section at $t = T_N/2$ for Case B. $\omega_0 = \pi$, $T_N = 1$, (c) $T_L = 0.3$, (d) $T_L = 0.35$. Red and green lines depict the unstable and stable manifolds.

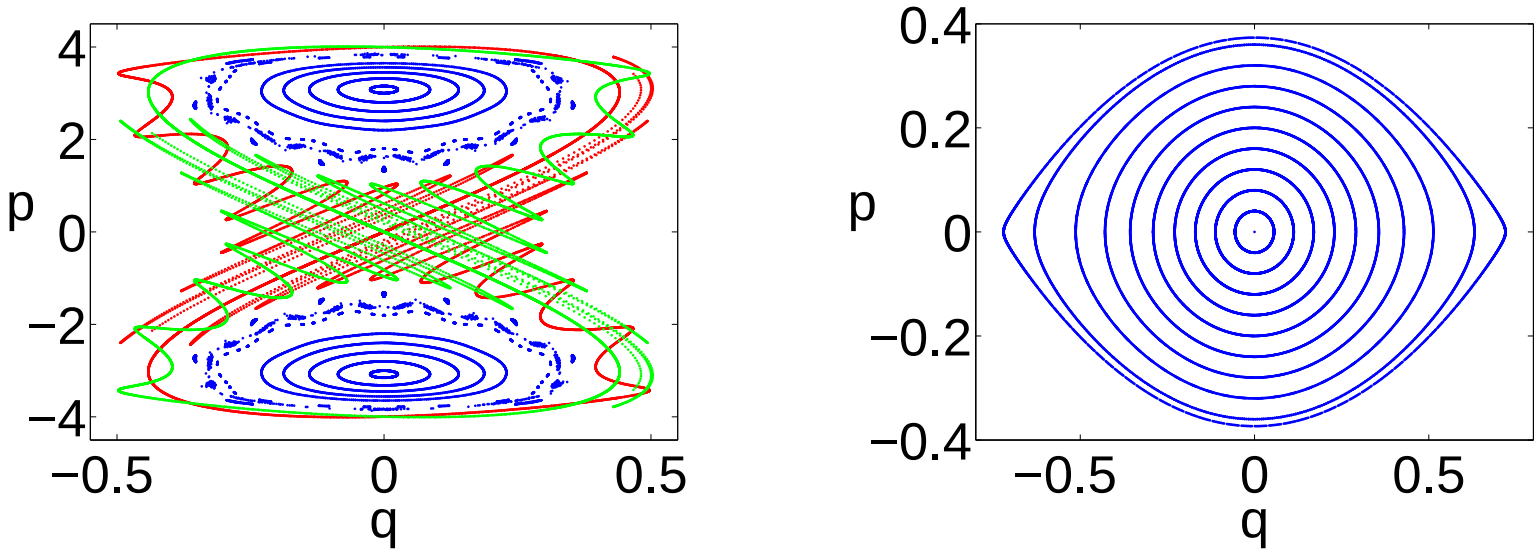

Figure 2 e,f: Poincare surface of section at $t = T_N/2$ for Case B. $\omega_0 = \pi$, $T_N = 1$, (e) $T_L = 0.37$, (f) $T_L = 0.95$. Red and green lines depict the unstable and stable manifolds.

Controlling solutions of non-autonomous lattices

The Hamiltonian describing particle dynamics in a lattice with an external on-site potential has the form

$$H = \sum_{n=1}^{N} \frac{1}{2} m \dot{y}_n^2 + \sum_{n=1}^{N} \Phi(y_n - y_{n-1}, t) + \sum_{n=1}^{N} \Phi_0(y_n, t) \qquad (5)$$

In the following we consider a case where the interaction potential in Eq. (5) has a time-dependent coefficient

$$\Phi(y_n - y_{n-1}, t) = u(t)\Psi(y_n - y_{n-1}) \qquad (6)$$

with u representing the effect of the time-varying external fields on the interaction potential.

More specifically, we focus on the case where **the interaction potential is periodically switched on-off**, so that $u(t)$ is a periodic piecewise constant function defined as

$$u(t) = \begin{cases} +1, & kT < t \leq kT + T_{+c} \\ 0, & kT + T_{+c} < t \leq kT + T_{+c} + T_u^{(1)} \\ -1, & kT + T_{+c} + T_u^{(1)} < t \leq kT + T_{+c} + T_u^{(1)} + T_- \\ 0, & kT + T_{+c} + T_u^{(1)} + T_{-c} < t \leq kT + T_{+c} + T_u^{(1)} + T_- \end{cases} \tag{7}$$

where $k = 0, \pm 1, \pm 2, \ldots$ The durations of the time intervals where the coupling is on and off are $T_{\pm c}$, $T_u^{(1,2)}$, respectively, and $T = T_{+c} + T_{-c} + T_u^{(1)} + T_u^{(2)}$ is the period of $u(t)$ (Fig.3). **In the coupled phase, the system evolves as in the autonomous lattice. In the uncoupled phase each particle oscillates independently in the external on-site potential.**

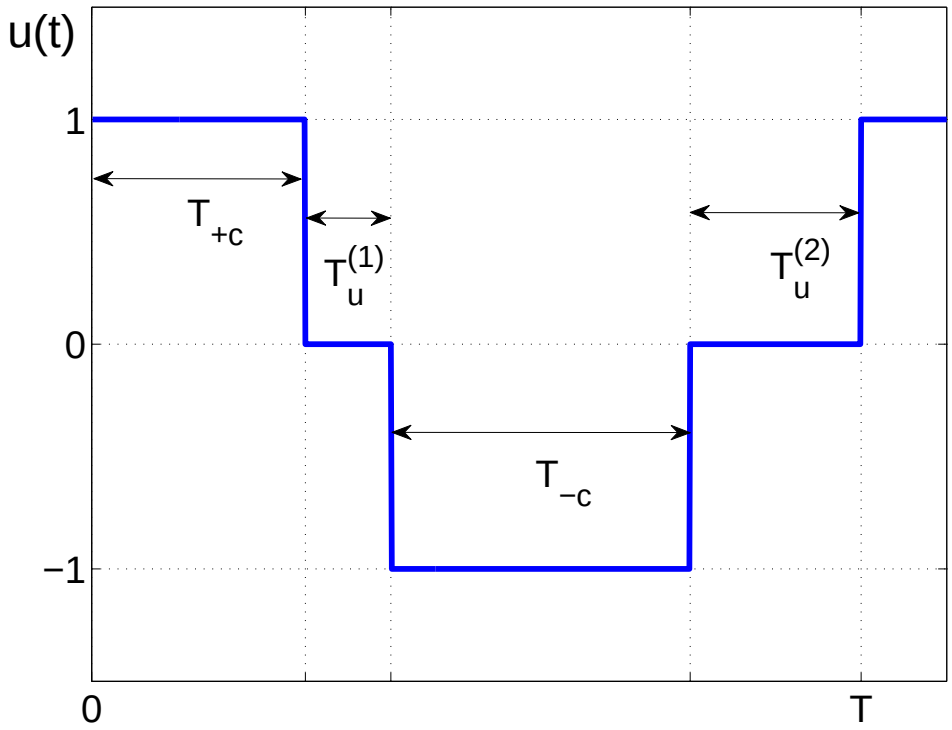

Figure 3: General form of the function $u(t)$.

Analytical Breather Solutions

We focus on the case where during the uncoupled phases, the external potential is of the form

$$\Phi_0(y_n, t) = v(t)\frac{\omega_0^2}{2}y_n^2 + u(t)\Psi_0^{(nl)}(y_n) \tag{8}$$

where $\Psi_0^{(nl)}(y_n)$ is a nonlinear on-site potential acting only at the coupled phase and $v(t) = 1 - u^2(t)$.

In the **uncoupled phases, every particle oscillates linearly** with frequency ω_0. When the durations of the uncoupled linear phases $T_u^{(1,2)}$ are integer multiples of the period of the oscillations, that is when

$$T_u^{(1,2)} = m^{(1,2)}2\pi/\omega_0, m = 1, 2, ... \tag{9}$$

the system, after the linear phase, returns exactly at the same state it was at the **end of the previous coupled phase**.

Controlling Solitons of the Toda Lattice

Let us focus on the integrable Toda lattice whose interaction potential is exponential:

$$\Psi(y_n - y_{n-1}) = e^{-(y_n - y_{n-1})} \tag{10}$$

Applying the canonical transformation from $(y_n, \dot{y}_n)$ to (r_n, s_n) where

$$r_n = y_n - y_{n-1} \tag{11}$$
$$\dot{y}_n = s_n - s_{n+1} \tag{12}$$

the Toda lattice solitons are given in the form

$$r_n^{sol}(t) = -\ln\left(\beta^2 \mathrm{sech}^2\left(\alpha n \mp \beta t\right) + 1\right) \tag{13}$$

where $\beta = \sinh(\alpha)$. These solitons move with a velocity $v_{sol} = \beta/\alpha$ which increases with the height of the pulse.

Following the previous arguments, under the condition (9), the respective solutions of the nonautonomous lattice can be written as

$$r_n(t) = \begin{cases} r_n^{sol}\left(t - k(T_{+c} - T_{-c})\right), & t \in \Delta T_1 \\ A_n^{(1,k)} \sin\left(\omega_0 t + a_n^{(1,k)}\right), & t \in \Delta T_2 \\ r_n^{sol}\left(-t + (1-k)T_{+c} + kT_{-c}\right), & t \in \Delta T_3 \\ A_n^{(2,k)} \sin\left(\omega_0 t + a_n^{(2,k)}\right), & t \in \Delta T_4 \end{cases} \tag{14}$$

with $\left(A_n^{(i,k)}, a_n^{(i,k)}\right)$, $i = 1, 2$ determined from matching conditions at the boundaries of the respective time intervals $t^{(i,k)}$ according to

$$A_n^{(i,k)} = \left([r_n^{sol}(t^{(i,k)})]^2 + \left[\frac{\dot{r}_n^{sol}(t^{(i,k)})}{\omega_0} \right]^2 \right)^{1/2} \tag{15}$$

$$a_n^{(i,k)} = \tan^{-1}\left(\frac{\omega_0 r_n^{sol}(t^{(i,k)})}{\dot{r}_n^{sol}(t^{(i,k)})} \right) \tag{16}$$

These solutions describe **localized waves propagating as Toda solitons when the coupling is on**, and **oscillate periodically when the coupling is off**. In the time interval when $u(t) = -1$ the soliton travels **in the opposite direction** in comparison to the interval when $u(t) = +1$, while the velocity of the wave is zero during the uncoupled phases. Therefore, the mean velocity of the wave is

$$< v >= \left(\frac{T_{+c} - T_{-c}}{T_{+c} + T_{-c} + T_u^{(1)} + T_u^{(2)}} \right) \frac{\beta}{\alpha} \qquad (17)$$

with $T_u^{(1,2)}$ taking one of the discrete values shown in Eq. (9). Thus, the periodically pulsating coupling results in **a "ratchet" effect on soliton (breather) dynamics**, since depending on the parameters of the function $u(t)$ it can decelerate the wave accordingly.

Firstly, let us consider the case where $u(t)$ takes the values $0, 1$ in the time intervals, $T_{-c} = T_u^{(2)} = 0$. In Fig. 4, the evolution of a breather having an initial form of a Toda soliton given by Eq. (13) with $\alpha = 1$, is shown for the case where $T_{+c} = 2$.

Fig. 4(a) depicts the evolution of an autonomous Toda soliton (this is equivalent to considering $m = 0$ in Eq. (9), and (b), (c), (d) a Toda lattice with periodically pulsating coupling with the duration of the uncoupled phase $T_u^{(1)}$ given by (9) for $m = 2, 3, 6$, respectively. The frequency of the uncoupled oscillations ω_0 is taken equal to 2π.

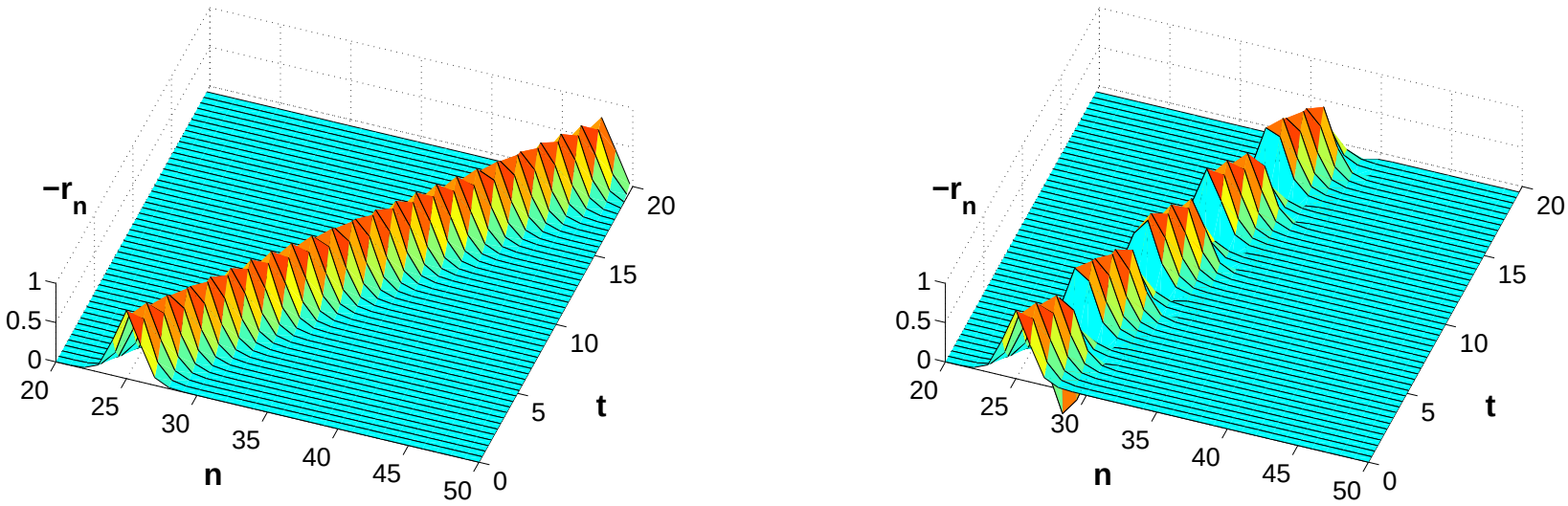

Figure 4 a,b: Evolution of a breather having an initial form of a Toda soliton with $\alpha = 1$ with $T_{-c} = T_u^{(2)} = 0$, $T_{+c} = 2$ and $T_u^{(1)} = m2\pi/\omega_0$ with $m = 0$ (a), $m = 2$ (b).

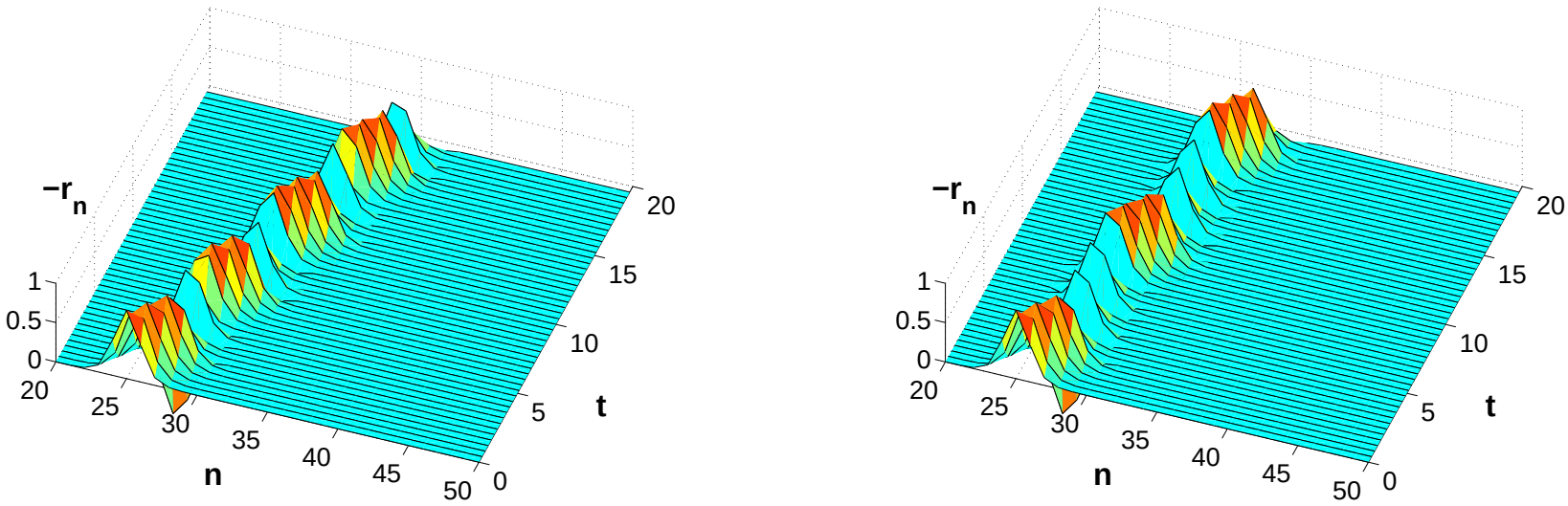

Figure 4 c,d: Evolution of a breather having an initial form of a Toda soliton with $\alpha = 1$ with $T_{-c} = T_u^{(2)} = 0$, $T_{+c} = 2$ and $T_u^{(1)} = m2\pi/\omega_0$ with $m = 3$ (c), $m = 6$ (d).

When condition (9) is **not met**, **the solitary wave deforms, splits and disperses** under propagation as shown in Fig. 5 for the case corresponding to a Toda soliton with $\alpha = 1$ and a $u(t)$ having $T_{-c} = T_u^{(2)} = 0,\ T_{+c} = 2,\ T_u^{(1)} = 2\pi/\omega_0 + 0.01$.

In Fig. 6, **collisions between two breathers with velocities of opposite sign** are shown for the case of two identical breathers corresponding to $\alpha = 1$ and $m = 1$ as well as two different breathers with $\alpha_1 = 1$, $\alpha_2 = 0.5$ and $m = 1$. The breathers undergo completely elastic collisions and remain intact.

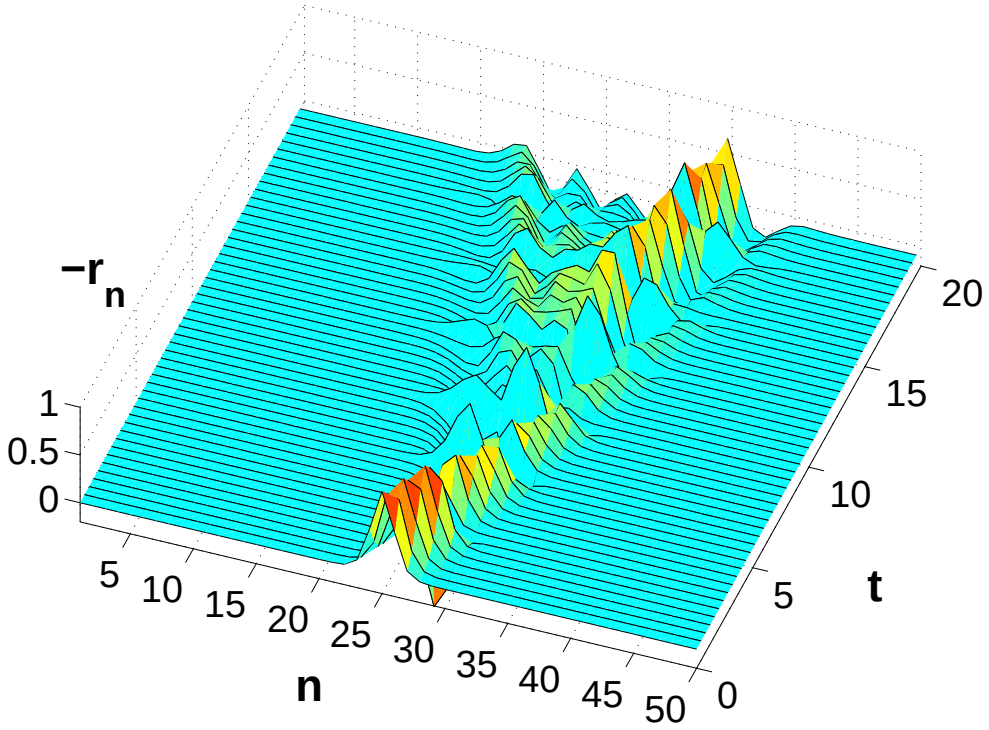

Figure 5: Evolution of an initial form as in Fig. 2(b), but with $T_u^{(1)} = 2\pi/\omega_0 + 0.01$.

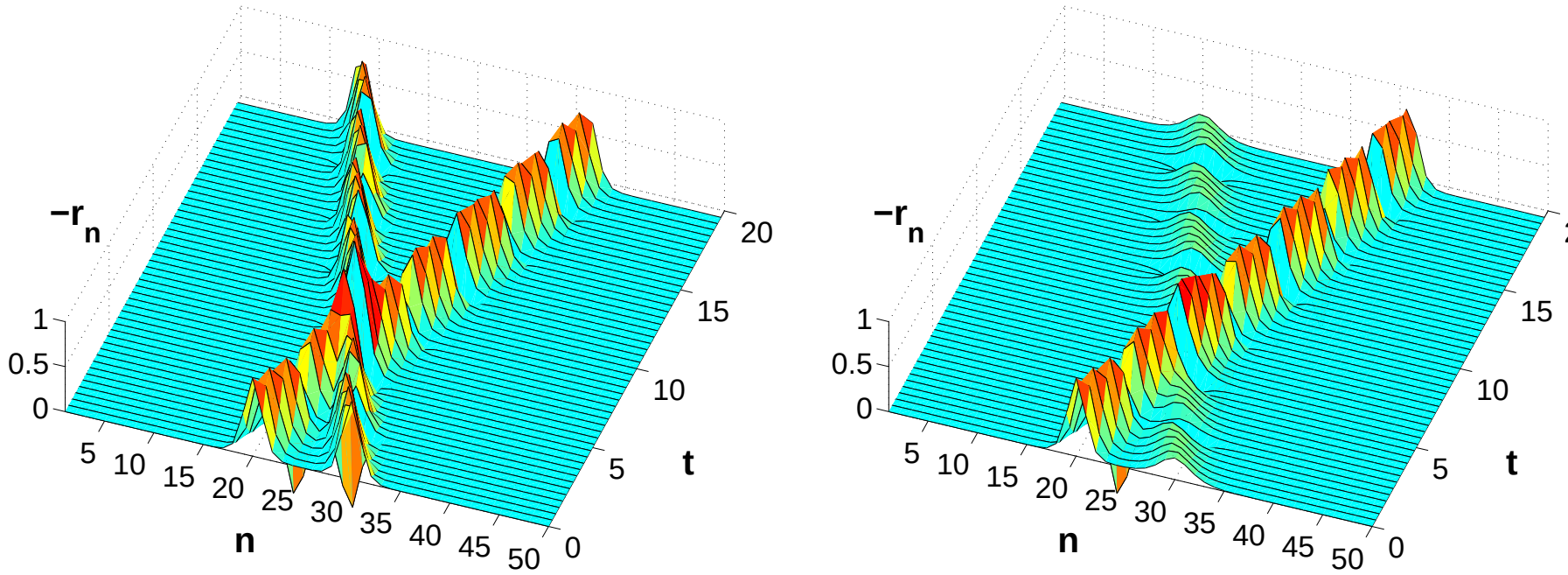

Figure 6: Collisions between two breathers with velocities of opposite sign corresponding to Toda solitons having (a) $\alpha_1 = \alpha_2 = 1$, (b) $\alpha_1 = 1, \alpha_2 = 0.5$. The parameters of the function $u(t)$ are $T_{-c} = T_u^{(2)} = 0$, $T_{+c} = 2$ and $T_u^{(1)} = 2\pi/\omega_0$.

In Fig. 7 we show the evolution of a Toda soliton for the case of a $u(t)$ taking the values $0, \pm 1$ in the respective time intervals. The durations of the uncoupled phases are $T_u^{(1)} = T_u^{(2)} = 2\pi/\omega_0$. Depending on the values of T_{+c} and T_{-c} **the breather can have a positive (Fig. 7(a)) or negative mean velocity** according to Eq. (17).

When $T_{+c} = T_{-c}$ **the mean velocity is zero** and the breather undergoes **a periodic "swinging" motion (Fig. 7(b))**. Moreover, **we can control breather collisions as shown in Fig. 8**, where depending on T_{+c} and T_{-c} we can either prevent collisions (Fig. 8(a)) or make two breathers collide periodically (Fig. 8(b)).

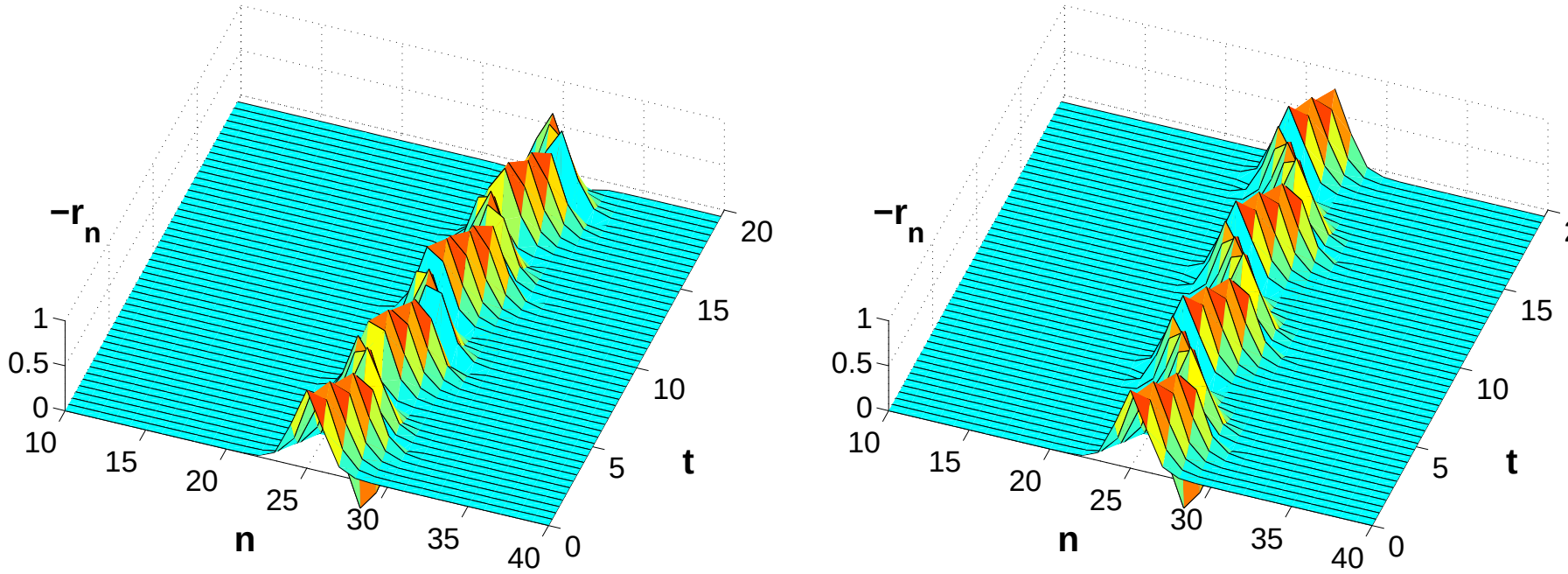

Figure 7: Evolution of a breather having an initial form of a Toda soliton with $\alpha = 1$ with $T_u^{(1)} = T_u^{(2)} = 2\pi/\omega_0$ and (a) $T_{+c} = 2, T_{-c} = 1$, (b) $T_{+c} = 1, T_{-c} = 2$, (c) $T_{+c} = 2, T_{-c} = 2$.

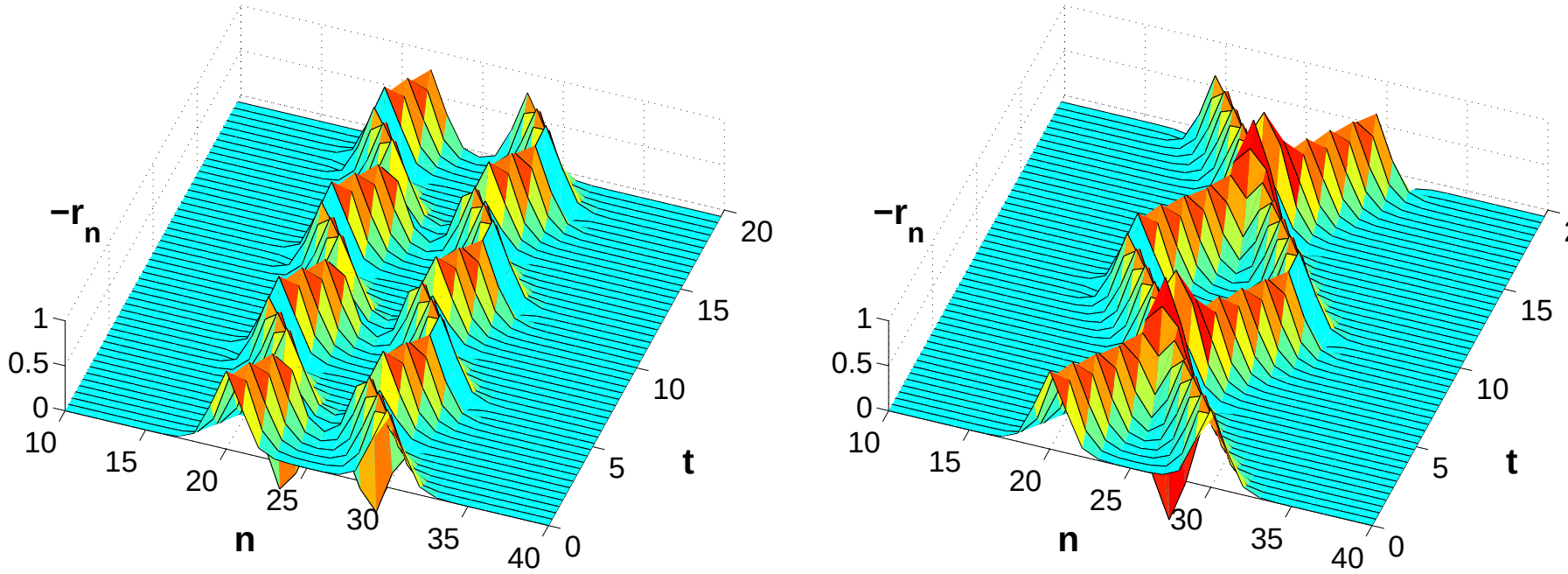

Figure 8: Evolution of two breathers corresponding to Toda solitons with $\alpha = 1$ with $T_u^{(1)} = T_u^{(2)} = 2\pi/\omega_0$ and (a) $T_{+c} = T_{-c} = 2$, (b) $T_{+c} = T_{-c} = 4$.

Non-paraxial Traveling Solitary Waves in Layered Nonlinear Media

Wave propagation in **inhomogeneous media** is one of the most ubiquitous phenomena occurring in almost every branch of physics. The inhomogeneity of a medium determines the **linear diffraction properties** so that appropriately designed spatial structures can have desirable propagation properties.

In **nonlinear materials**, spatial self-localization of the waves leads to **Solitary Waves (SW) and solitons**. **The combination of the inhomogeneity and nonlinearity, in nonlinear optics**, has led to theoretical and experimental studies in photonic structures of varying complexity such as photonic crystals, waveguide arrays and periodic or disordered lattices, where **effective light control** is of the utmost importance.

The dominant underlying model governing SW formation and propagation in such structures is the **NonLinear Schrödinger equation (NLS)**,

$$i\psi_z + \psi_{xx} + \epsilon(x)\psi + g(x, |\psi|^2)\psi = 0, \tag{18}$$

where z,x and ψ are the propagation distance, transverse direction and electric field respectively. It is derived from Maxwell's equations under the so-called **paraxial approximation**:
(i) **the beam width is much larger than the wavelength** (slowly varying envelope approximation),
(ii) **the beam propagates primarily along the z - axis**.
These conditions restrict drastically the domain of applicability of the NLS equation.

How can we do better?

For the case of **layered media**, Maxwell's equations, **lead without approximation** to a scalar **NonLinear Helmholtz (NLH) equation** with an intensity-dependent refractive index, when the electric field is assumed to be monochromatic and linearly polarized along the y direction.

$$E_{zz} + E_{xx} + \beta^2(x)E + \gamma(x)|E|^2 E = 0 \tag{19}$$

where the electric field E is normalized to E_0, $\beta \equiv n_0\omega/c$, $\gamma \equiv 2(n_2 E_0^2/n_0)\beta^2$ and $n_0(x)$, $n_2(x)$ are the linear and nonlinear refractive indices that we will take to be **piecewise constant functions** of the transverse coordinate x.
The NLS and NLH equations have **fundamentally different** mathematical properties resulting in the description of qualitatively different phenomena of wave propagation.

Analytical solutions for traveling SW of the NLH equation

Traveling wave solutions of the NLH Eq. (19) can be sought in the form

$$E(x,z) = u\left(x - x_0(z)\right) e^{i(k_x x + k_z z)} \tag{20}$$

where u is real transverse wave profile, and k_x, k_z are the transverse and longitudinal wavenumbers. Substitution of Eq. (20) in Eq. (19) results in an ODE for the transverse wave profile

$$u_{xx} + \frac{\beta^2(x) - k^2}{1+v^2} u + \frac{\gamma(x)}{1+v^2} u^3 = 0 \tag{21}$$

with $k^2 \equiv k_x^2 + k_z^2$, $v \equiv dx_0/dz = k_x/k_z$ being the transverse wave velocity corresponding to a propagation angle $\theta = \tan^{-1}(k_x/k_z)$. Recall that $\beta(x), \epsilon(x)$ are **piecewise constant** functions.

For a **homogeneous nonlinear medium** (where β, γ are constants) there exist a homoclinic (heteroclinic) solution for every x_0 provided that $k^2 > \beta^2$ ($k^2 < \beta^2$) and $\gamma > 0$ ($\gamma < 0$):

$$u = \sqrt{2\frac{k^2-\beta^2}{\gamma}}\,\mathrm{sech}\left(\sqrt{\frac{k^2-\beta^2}{1+v^2}}(x - x_0(z))\right) \tag{22}$$

$$u = \sqrt{\frac{k^2-\beta^2}{\gamma}}\tanh\left(\sqrt{\frac{\beta^2-k^2}{2(1+v^2)}}(x - x_0(z))\right) \tag{23}$$

These solutions travel with transverse velocity v. **In the paraxial limit $v^2 \ll 1$ (22) and (23) correspond to the bright and dark soliton solutions of the NLS equation respectively**.

The importance of layered structures

As with the Kronig-Penney model, we can study layered structures consisting of **interlaced linear and nonlinear** parts described by the refractive index profiles

$$[n_0(x), n_2(x)] = \begin{cases} \left(n_0^l, 0\right), & x \in U_L \\ \left(n_0^{nl}, n_2\right), & x \in \mathbb{R} - U_L \end{cases} \tag{24}$$

where $U_L = \bigcup_m [N/2 + (m-1)T, N/2 + (m-1)T + L]$ with $m = 1, 2, ...M$ is the union of the linear parts with $T = L + N$ and L, N being the lengths of the linear and the nonlinear layers, respectively.

The transverse profile of the wave is described by Eq. (21) with $\beta = \beta_l \equiv n_0^l \omega/c$, $\gamma = 0$ and $\beta = \beta_{nl} \equiv n_0^{nl} \omega/c$, $\gamma \neq 0$ in the linear and nonlinear parts, respectively.

t We choose $k^2 < \beta_l^2$ so that **he solutions of Eq. (21) within the linear parts are periodic**, while in the nonlinear parts we have $k^2 > \beta_{nl}^2$ ($k^2 < \beta_{nl}^2$) and $\gamma > 0$ ($\gamma < 0$) so that the bright (dark) SW solution given by Eq. (22) [Eq. (23)] exist.

The total wave profile can be obtained by **matching the boundary conditions between subsequent layers**. When $k^2 > \beta_{nl}^2$ performing this for the bright solitona on a structure with $M = 1$ layer leads to **a resonance condition valid all** x_0

$$k^2 = \beta_l^2 - \left(\frac{n\pi}{L}\right)^2 (1 + \tan^2\theta), \quad n = 1, 2, ... \tag{25}$$

This is a family of solutions for every n, and includes symmetric, antisymmetric and an infinite number of asymmetric modes. It allows for **the existence of traveling SW solitary waves for every** $x_0(z) = vz + x_0(0)$ **in contrast to the general case where only standing SW exist, at fixed** x_0.

The condition (25)represents a spatial resonance according to which an integer number of half-periods of the sinusoidal wave profile in the linear part is contained within the length of the linear part L.

Under Eq. (25), **any solution starting from a point of the homoclinic (heteroclinic) orbit at the boundary** between a nonlinear and a linear component **returns to the same point** (for n, even) or **to its symmetric point with respect to the origin** (for n, odd) after evolving with respect to x in the linear part of length L.

Thus, the propagation of a SW may be described as **reflectionless transmission** in a structure consisting of **a single linear layer and one consisting of 3 layers is depicted in Figures 9 and Figure 10**.

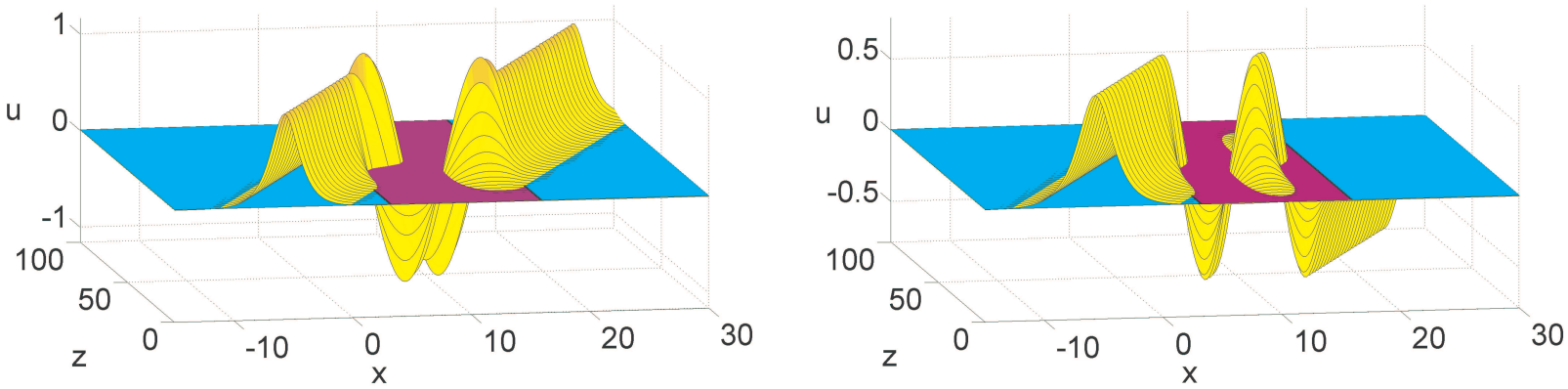

Figure 9: Traveling of a bright SW in a structure consisting of a single linear layer ($M = 1$) with $L = 4\pi$, $N = 2\pi$. The velocity is $v = 0.2$ and $n = 2$ (left), 3 (right). $\gamma = 2$, $\beta_{nl}^2 = 0.3$, $\beta_L^2 = 1.5$.

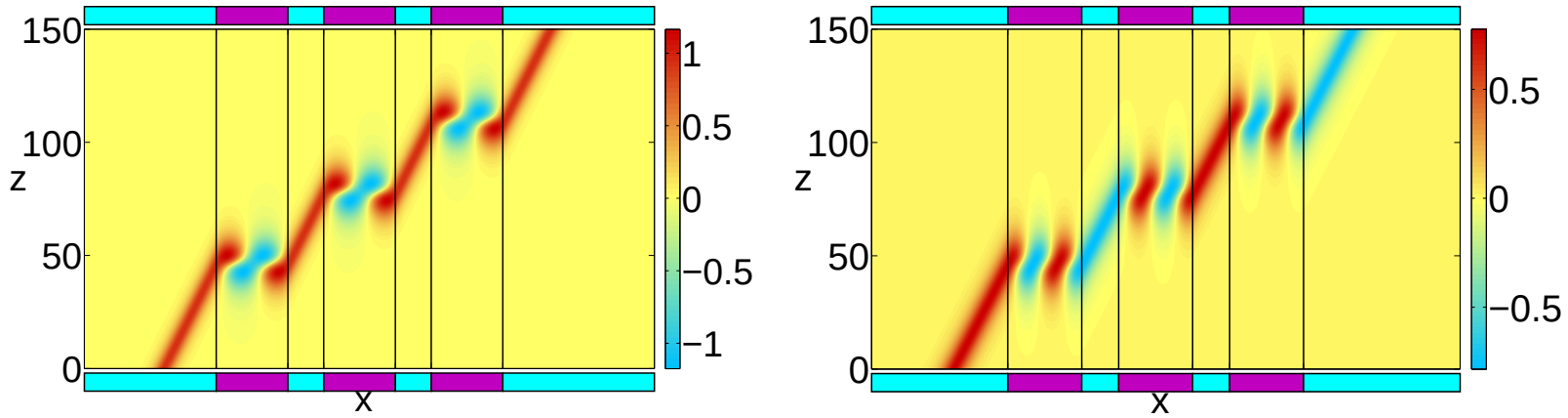

Figure 10: Traveling of a bright SW in a structure consisting of three linear layers ($M = 3$). All other parameters are the same with those of Figures 7, 8.

Conclusions

1. We have studied a class of **nonautonomous piecewise linear systems** that consist of **a periodic sequence of linear and nonlinear autonomous components** each acting alone in a different time (or space) interval. We focused on the investigation of **control capabilities** of such systems by changing their phase space structure.

2. Choosing appropriately **the length of the linear and nonlinear intervals**, we showed that it is possible to **continue exactly analytical solutions** of the nonlinear component by matching the respective solutions at the boundaries with the linear intervals.

3. As a first example, we considered the case of a **one-degree-of freedom Duffing equation**, with periodically switched on-off coefficients, and showed that homoclinic (heteroclinic) solutions can be continued analytically across the linearly periodic regime.

4. In the case of **a non-autonomous Toda lattice with periodically switched nearest-neighbor coupling**, the solitons become breathers and a "ratchet" effect occurs as a result of deceleration, **providing a mechanism for breather velocity and collision control.**

5. Applications to **problems of nonlinear optics** were discussed: In particular, we have obtained a large class of **exact traveling Solitary Wave (SW) solutions for a variety of inhomogeneous structures consisting of linear and nonlinear layers**. These solutions describe reflectionless and radiationless SW propagation for arbitrary angles and spatial widths **in the non-paraxial regime**.

6. The generality of the results facilitates the **experimental observation** of such SW solutions in **planar dielectric structures** in the form of finite or infinite waveguide arrays.

References

1. Y. Kominis and T. Bountis, "Analytical Solutions of Systems with Piecewise Linear Dynamics", Int. J. Bifurc. Chaos 20, Issue: 2, 509-518 (2010).

2. Y. Kominis, T. Bountis, and K. Hizanidis, "Breathers in a Nonautonomous Toda Lattice with Pulsating Coupling", Phys. Rev. E 81, 066601 (2010).

3. Yannis Kominis, Tassos Bountis and Kyriakos Hizanidis, "Complex Dynamics of Piecewise Linear Systems: Theory and Applications", Proceedings of 10th Congress HSTAM, Chania, Crete, 25-27 of May, 2013.

4. Yannis Kominis, "Non-paraxial Traveling Solitary Waves in Layered Nonlinear Media", preprint submitted for publication (2013).